# Bluntnose Sixgill Shark (*Hexanchus griseus*)

**Supplementary Information for *Hexanchus griseus***

To analyse the Bluntnose Sixgill Shark population trend data, we used a generalized Bayesian state-space model tool for trend analysis of abundance indices for IUCN Red List assessment (Just Another Red List Assessment, JARA) (Sherley *et al.* 2020, Winker et al. 2020). The relative abundance assessment of the population follows an exponential state-space population model of the form: $\mu_{t+1} = \mu_t + r_t$, where $\mu_t$ is the logarithm of the expected abundance in year *t,* and $r_t$ is the normally distributed annual rate of change with mean $\bar{r}$, the estimable mean rate of change for a population, and process variance $\sigma^2$. We linked the logarithm of the observed relative abundance $y_{t,i}$ in year *t* for index *i* (where multiple indices were available for the same fishery or region) to the expected but unobserved abundance $\mu_t$ in year *t*, $\log(y_{t,i}) = \mu_t + \log(q_i) + \varepsilon_{t,i}$, where $q_i$ is a scaling parameter (catchability) for index *i.* The abundance index with the oldest record (in order of occurrence) is taken as a reference index by fixing $q_i = 1$ and the other indices are scaled to this reference index, respectively, with $q_{2...n}$ being estimable model parameters. We used a non-informative normal prior for $\bar{r} \sim N(0,1000)$. Priors for the process variance can be either fixed or estimated (see Winker *et al.* 2020 for details). If estimated (default), the priors were $\sigma^2 \sim 1/gamma$ (0.001,0.001), or approximately uniform on the log scale (e.g. Chaloupka and Balazs 2007). Two Monte Carlo Markov chains were run and initiated by assuming a prior distribution on the initial state centred around the first data point in each abundance time series ($y_{t=1}$), $\mu_1 \sim N(\log(y_1),1000)$. The first 1000 iterations of each chain were discarded as burn-in, and of the remaining 10,000 iterations, 5,000 were selected for posterior inference. Thus, posterior distributions were estimated from 20,000 iterations. Analyses were performed using the R Statistical Software v3.5.0 (R Core Team 2018), via the interface from R ('r2jags' library v 0.5-7; Su and Yajima 2015) to JAGS ('Just Another Gibbs Sampler' v4.3.0; Plummer 2003). Convergence was diagnosed using Geweke's diagnostic (Geweke 1992) with thresholds of $p = 0.05$, via the 'coda' library (v0.19-1; Plummer *et al.* 2006). The estimated posterior of the population trend for year *t* is then given by $\hat{I}_t = \exp(\mu_t)$.

The percentage change *D%* was directly calculated from the posteriors of the estimated population time series $\hat{I}_t$. If the span of $\hat{I}_t$ was longer than 3 x generation length (GL), the percentage change was automatically calculated as the difference between a three-year average around the final observed data point *T*, and a three-year average around the year corresponding to *T*−(3 × GL). The year *T+1* is always projected to obtain a three-year average around *T*. We used a three-year average to reduce the influence of short-term fluctuation (Froese *et al.* 2017). If the span of $\hat{I}$ was shorter than 3 × GL, JARA projected forward, by passing the number of desired future years without observations to the model, to attain an $\widehat{\hat{I}_t}$ that spans 3 × GL + 2 years for the calculation of *D%*. These projections (shown as red dashed lines in the figures below) were based on the posteriors of the estimated population reduction across all *n* years in the observed time series: $\bar{r} = \frac{1}{n}\sum_{t=1}^{n} r_t$.The

projection gives similar results to extrapolating backwards to attain a 3 x GL period and produces a similar result for the D%.

We analysed the time series for the region where data was available, to produce a) a model fit to the observed data (e.g. Figure 1a), b) an annual rate of change ($\lambda$) based on the observed data ($\lambda = \exp(\bar{r})$, expressed as a % in e.g. Figure 1b), c) if needed, projected values for each year necessary to extend the time-series to 3 × GL (e.g. Figure 1c), and d) the posterior distribution for the regional rate of change (%) over 3 × GL (e.g. Figure 1d). Because the posterior distribution comprises an estimated % population change over 3 × GL for each model iteration, these automatically map to the IUCN Red List categories. For example, under criterion A2, an iteration yielding a % population change of +55% would be assigned to the Least Concern category, while iterations giving −82% and −55% would be assigned to Critically Endangered and Endangered, respectively. This probable Category was then used by assessors to inform the species' status while considering other available information that was not included in this analysis (i.e. there is other information beyond timeseries and this JARA analysis that needs to be considered to arrive at a Category, and the final Category may not exactly reflect what JARA suggests).

**Northeast Atlantic:** Nominal CPUE, trawl (kilogram of sharks per hour) (F. Neat unpubl. data 2019) and relative biomass, trawl (kg per haul) (ICES 2018: Figure 5.11 (top), page 189) (1998–2019).

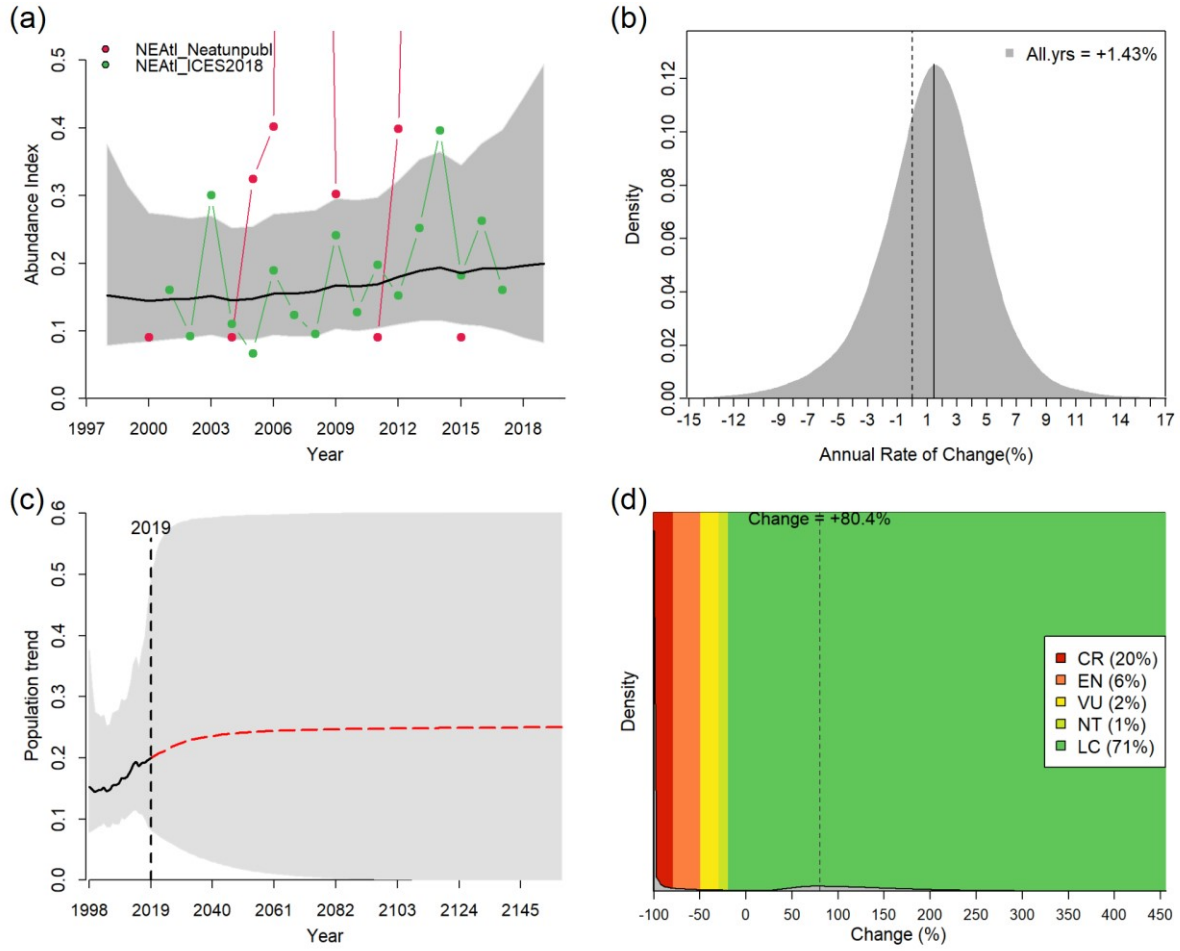


**Figure 1.** JARA results for the Bluntnose Sixgill Shark (*Hexanchus griseus*) in the Northeast Atlantic Ocean showing (a) the JARA fit to the observed time-series, (b) the posterior probability for the percentage annual population change calculated from all the observed data (in grey) shown relative to a stable population (% change = 0, black dashed line), (c) the observed (black line) and predicted (red line) population trajectory over three generations (160 years, dashed lines) and (d) the median reduction over three generation lengths and corresponding probabilities for rates of population reduction falling within the IUCN Red List categories.

## References


Chaloupka, M. and Balazs, G. (2007) Using Bayesian state-space modelling to assess the recovery and harvest potential of the Hawaiian green sea turtle stock. *Ecological Modelling* **205**: 93–109.

Froese, R., Demirel, N., Coro, G., Kleisner, K.M. and Winker, H. (2017) Estimating fisheries reference points from catch and resilience. *Fish and Fisheries* **18**: 506–526.

Geweke, J. (1992) Evaluating the accuracy of sampling-based approaches to the calculation of posterior moments. In: *Bayesian Statistics 4: Proceedings of the Fourth Valencia International Meeting.* (eds J.O. Berger, J.M. Bernardo, A.P. Dawid and A.F.M. Smith).

Plummer, M. (2003) *JAGS: A Program for Analysis of Bayesian Graphical Models using Gibbs Sampling*, (Vol. 124).

Plummer, M., Nicky Best, Cowles, K. and Vines, K. (2006) CODA: Convergence Diagnosis and Output Analysis for MCMC. *R News* **6**: 7–11.

Sherley, R.B., Winker, H., Rigby, C.L., Kyne, P.M., Pollom, R., Pacoureau, N., Herman, K., Carlson, J.K., Yin, J.S., Kindsvater, H.K., and Dulvy, N.K. (2020) Estimating IUCN Red List population reduction: JARA—A decision-support tool applied to pelagic sharks. Conservation Letters, e12688. doi: 10.1111/conl.12688.

Su, Y.-S. and Yajima, M. (2012) R2jags: A Package for Running jags from R.

Winker, H., Carvalho, F. and Kapur, M. (2018) JABBA: Just Another Bayesian Biomass Assessment. *Fisheries Research* **204**: 275–288.

Winker, H., Pacoureau, N., and Sherley, R. B. (2020) JARA: 'Just Another Red list Assessment'. *bioRxiv* 672899 doi:10.1101/672899.